Environmental Engineering and Management Journal

June 2019, Vol. 18, No. 6, 1311-1325
http://www.eemj.icpm.tuiasi.ro/; http://www.eemj.eu

"Gheorghe Asachi" Technical University of Iasi, Romania

ASSESSMENT MODEL OF STRATA PERMEABILITY CHANGE DUE TO UNDERGROUND LONGWALL MINING

Jianwei Cheng[1,2*], Chang Qi[3], Weidong Lu[2], Kaixuan Qi[3]

[1]State Key Laboratory of Coal Resources and Safe Mining, China University of Mining and Technology, Xuzhou, Jiangsu, 221116, China
[2]Department of Safety Engineering, Xin Jiang Institute of Engineering Urumqi, Xinjiang, 830000, China
[3]School of Safety Engineering, China University of Mining and Technology, Xuzhou, Jiangsu, 221116, China

Abstract

The coal gas is a potential risk for the safety production in coalmines. The practical experiences in coalmine show that the gas may suffer massive desorption and migration after coal seam mining and deformation of overlying strata. Therefore, gas extraction in mines focuses on mining ground pressure relief gas extraction. In this paper, the study is carried out on gas permeability and migration pathway based on movements of overlying strata over the working face and the spatial location of the coal gas enrichment area. 3D prediction models for overlying strata subsidence of the working face are developed to analyze the movement and deformation law of overlying strata. The concept of "total strain" is introduced to describe the fracture development of overlying strata. The relationship between "total strain" and porosity and permeability are further established. The distribution law of the mining permeability change under final subsidence of overlying strata is analyzed to scientifically reveal the permeability change and migration pathway of gas. The accurate "annular" location of the gas enrichment area in overlying strata is identified. The developed model provides important theoretical guidance for designing parameters of optimized gas drainage system and to improve efficiency extraction of coal seam gas.

Key words: mining subsidence, permeability, porosity, subsurface strata deformation, total strain

Received: August, 2017; Revised final: February, 2018; Accepted: March, 2018; Published in final edited form: June 2019

1. Introduction

Because of untouchability and invisibility of overlying strata of an underground mining working face, movement and deformation law of surface and overlying strata subsidence under the influence of mining is a very complicated process, and the theoretical research and prediction aiming at such process are always highly concerned by researchers. The basic law of the surface movement in coalmine was analyzed by some authors whomarked the beginning of systematic study on mining subsidence process science (Liu and Liao, 1965; Liu, 1992; Liu and Lin, 1982). He (1988) firstly put forward the skew mathematical expression of "Weibull distribution" of surface subsidence basin in the mine; Zhang et al. (1987) proposed the dislocation theory and the boundary element method related to ground strata movement; Qian et al. (2010) innovatively put forward the "masonry beam theory" related to subsidence of overlying strata; Deng (1999) presented the structure effect because of mining subsidence engineering; the study on the distribution of overlying strata joint of the coal seam using the physical simulation approach carried by Xie et al. (1998) shows that the existence of joint results in intensified damage to overlying strata of coal seam and controls the development of fractures in mining overlying strata; Guo et al. (2011) carried out field observations of ground subsidence caused by the top coal caving with

* Author to whom all correspondence should be addressed: e-mail: Cheng.Jianwei@cumt.edu.cn; Phone: +86-189-5211-0121; Fax: +86-516-8359-0598

a large thick coal seam and analyses the basic subsidence law; Donnelly et al. (2001) integrated various factors, such as mining thickness of coal seam, thickness of overlying strata, dip of coal seam, and length of working face, into SWIFT software developed by Department of Mining Engineering of Nottingham University. It can make the quantitative prediction range of subsidence of overlying strata in gob. The CISPM software for prediction of surface subsidence of coal mining working face was developed by Peng and Luo (1992) using influence function method is widely used. Researchers also combined the Knothe theory based on probability integral method and used the so-called closed loop integration method of polar coordinates to develop the mathematical subsidence prediction model for overlying strata in gob. The model can carry out mining subsidence prediction over any gob shapes. In addition, other scholars also developed the subsidence prediction method based on theory of elasticity and theory of plasticity, for example, damage finite element method (Deng, 1999); fuzzy finite element method (Zhang, 1996); non-linear smooth finite element method (He, 1996); destruction non-linear large deformation finite element method (Xie and Chen, 1988), which provide new ideas for accurate prediction of mining subsidence in mines.

The change in stress-strain of overlying strata of coal mining working face under the influence of mining and the evolution of the permeability of coal strata have important guidance significances to coal gas drainage in the working face. Researchers carry out massive studies and obtain many research findings. Mostofa and Quamruzzaman (2009) carried out study on distribution law of mining stress of the working face with C++ programming language based on Wilson empirical equation aiming at the s coal seam mining in Bangladesh; Schatze et al., (2012) carried out test on the change in permeability of overlying strata caused by mining coal seam with using segmented water pressure test and point out the change law of the permeability of overlying strata within range of 24~46m in front of working face; Jiang pointed out that the cubic polynomial relation exists between effective stress and permeability, which is validated by the experiment (Jiang et al., 1997); Xue et al. (2013) studied the evolution law of rock volume expansion and gas permeability in the advancing process of the working face and obtain that the evolution distribution of both has consistency and point out the permeability evolution of the upper protective coal seam layer falls behind the evolution of the permeability of the protective layer; Researchers found that if the gas pressure in coal strata is larger, the swelling deformation of coal and rock is larger, the porosity is smaller, and the permeability of gas in coal strata is smaller through the analysis of the relationship between swelling deformation and porosity and permeability under the gas adsorption and deformation of coal and rock skeleton (Li et al., 2005; Tošović et al., 2016; Wang et al., 2012); In addition, similar change law exists between stress-strain curve and strain-permeability curve of coal and rock through permeability test and CT screening test in the stress-strain process is also pointed out. The permeability of coal and rock presents the property of strain hysteresis (Han et al., 2010; Minea and Croitoru, 2017; Zhao and Meng, 2010).

In this paper, considering the deformation characteristics of overlying strata, a mathematical model that could calculate the subsurface strata movements is developed, Further, the comprehensive model of strain-porosity-permeability for strata under mining is also derived. In order to demonstrate the model, a case study of the assessment of porosity/permeability change after mining is showed. Based on the calculation results, a plan of gas drainage is detail designed, which is good for engineering practices in the future.

2. Mathematical model overview

2.1. Development of prediction model for subsidence of overlying strata due to underground coal mining

The prediction of surface migration and deformation in a coal mine has important significances to surface deformation and damage caused by the influence of mining in the process of reducing coal mining. At present, relevant researchers carry out extensive researches on the prediction of surface movement and deformation and achieve the good results. So far, researchers study and develop various prediction methods of surface subsidence, mainly including: prediction method based on field observation experiences (including graphic method, section function method, etc.), prediction method based on influence function (typical as Knothe influence function) and theoretical model method (including stochastic medium theory, finite element method, discrete element method and boundary element method based on theory of elasticity and theory of plasticity). Because the calculation parameters used by the influence function method are obtained from field measured data and this method is applicable to various mining methods, gob shapes and prediction of displacement of any point on the surface, which has become one of the important methods successfully and widely used in the prediction of surface subsidence in mines. The brief introduction to the influence function method aiming at the prediction of surface subsidence is made below.

The influence function methods employ a cause-oriented approach in subsidence prediction. It states that the extraction of an elemental area of an underground coal seam will cause surface to subside in a particular manner. For level or moderately inclined coal seam, the surface point located directly above the extracted element receives the most amount of subsidence. The further the surface point is away from the extracted element, the less amount of influence received at the surface point.

The Knothe's influence function is the most successful one that has been adapted by many of the

major coal producing countries. It states that the distribution of the subsidence caused by the extraction of one unity area can be expressed by a modified normal probability distribution function. The influence for subsidence in a two dimensional case is shown in (Eq. 1):

$$f_s(x') = \frac{S_{\max}}{R} e^{-\pi(\frac{x'}{R})^2} \tag{1}$$

$$S_{\max} = ma \tag{2}$$

In Eq. (2): $S_{\max}$ is the maximum possible subsidence, m; m is the mining height, m; a is the subsidence factor, R is the radius of major influence, m; x' is the horizontal distance between the extracted element and the surface point where final subsidence to be calculated, m.

Based on the basic principle of the influence function method, it is easy to generalize the prediction equation of 2-D subsidence to the general 3-D case. In this paper, the expression of the influence function of surface subsidence prediction in the 2-D case (Eq. 1) is obtained and the expression of the influence function of the subsidence prediction in three dimensions is obtained as (Eq. 3):

$$f_s(x', y') = \frac{S_{\max}}{R^2} e^{-\pi(\frac{x'^2+y'^2}{R^2})} \tag{3}$$

The mathematical expressions of horizontal influence function along the X axis and the Y axis are obtained as (Eq. 4) and (Eq. 5):

$$f_{ux}(x', y') = -2\pi \frac{S_{\max}}{R^2 \cdot h} x' e^{-\pi(\frac{x'^2+y'^2}{R^2})} \tag{4}$$

$$f_{uy}(x', y') = -2\pi \frac{S_{\max}}{R^2 \cdot h} y' e^{-\pi(\frac{x'^2+y'^2}{R^2})} \tag{5}$$

The final subsidence S(x, y) at the prediction point (x, y) is obtained by integrating the 3-D influence function for subsidence (Eq. 3). The computing area is defined by pulling a distance equivalent to the offset of inflection point (d) back from the actual boundary of the mine gob. In order to make the method flexible, different d's are assumed along the four edges of the rectangular mine gob. In order to simplify the mathematical model, a local coordinate system (X'-O'-Y') is set. The origin is placed at the prediction point. The mathematical expression of final subsidence at the prediction point shown in (Eq. 6).

$$S(x, y) = \frac{S_{\max}}{R^2} \iint e^{-\pi(\frac{x'^2+y'^2}{R^2})} dA \tag{6}$$

$$S(x, y) = \frac{S_{\max}}{R^2} \int_{d_1-x}^{L-d_2-x} e^{-\pi(\frac{x'}{R})^2} dx' \cdot \int_{d_3-y}^{W-d_4-y} e^{-\pi(\frac{y'}{R})^2} dy' \tag{7}$$

Applying the knowledge mentioned in the previous section, the expression for final subsidence can be re-written into the following (Eq. 7) and (Eq. 8). The finial subsidence parameters (subsidence factor a, radius of major influence R and offset of inflection point d in above equations should be linked the vertical distance between the point of interest and the mined coal seam (h). They are noted as $a(h)$, $R(h)$ and $d(h)$. Therefore, the finial subsidence and horizontal displacement are expressed by Eqs. (9 - 11).

$$S(x, y, h) = \frac{a(h) \cdot m}{R(h)^2} \int_{d(h)-x}^{L-d(h)-x} e^{-\pi(\frac{x'}{R(h)})^2} dx' \cdot \int_{d(h)-y}^{W-d(h)-y} e^{-\pi(\frac{y'}{R(h)})^2} dy' \tag{8}$$

$$U_x(x, y, h) = \left[2\pi \frac{a(h) \cdot m}{R(h) \cdot h} \int_{d(h)-x}^{L-d(h)-x} x' e^{-\pi(\frac{x'}{R(h)})^2} dx' \right] \cdot \left[\frac{1}{R(h)} \int_{d(h)-y}^{W-d(h)-y} e^{-\pi(\frac{y'}{R(h)})^2} dy' \right] \tag{9}$$

$$U_y(x, y, h) = \left[2\pi \frac{a(h) \cdot m}{R(h) \cdot h} \int_{d(h)-y}^{W-d(h)-y} y' e^{-\pi(\frac{y'}{R(h)})^2} dy' \right] \cdot \left[\frac{1}{R(h)} \int_{d(h)-x}^{L-d(h)-x} e^{-\pi(\frac{x'}{R(h)})^2} dx' \right] \tag{10}$$

The vertical strain is the first order derivative of subsidence of overlying strata with respect to '$-h$', namely (Eq. 12),

$$\varepsilon_z(x,y,h) = -\frac{dS(x,y,h)}{dh} \tag{11}$$

The horizontal strain in X-axis direction and Y-axis direction is the first order derivative of horizontal movement in the corresponding direction, namely (Eq. 13) and (Eq. 14).

$$\varepsilon_x(x,y,h) = \frac{dU_x(x,y,h)}{dx} \tag{12}$$

$$\varepsilon_y(x,y,h) = \frac{dU_y(x,y,h)}{dy} \tag{13}$$

Under 3D condition, the total strain of mining overlying strata can be considered as volume strain. According to mathematical equation of volume strain, the mathematical expression of total strain of overlying strata under 3D condition can be obtained as (Eq. 15):

$$\varepsilon_t(x,y,h) = \varepsilon_x(x,y,h) + \varepsilon_y(x,y,h) + \varepsilon_z(x,y,h) \tag{14}$$

where: $a(h)$ indicates the subsidence coefficient of overlying strata; $R(h)$ indicates the main influence radius of mining overlying strata, m; $d(h)$ indicates the displacement distance of inflection point of overlying strata, m; m indicates the mining thickness of the coal seam, m; W indicates the dip width of gob, m; L indicates the strike length of gob, m; h indicates the height above the coal seam, m; x indicates the x-axis coordinate of predicted point of overlying strata in global coordinate system, m; y indicates the y-axis coordinate of predicted point of overlying strata in global coordinate system, m; x' indicates the distance between mining unit of coal seam in local coordinate system and predicted point of overlying strata in x'-axis direction, m; y' indicates the distance between mining unit of coal seam in local coordinate system and predicted point of overlying strata in y'-axis direction, m. Therefore, Eqs. (9-15) are prediction models for finial subsidence of overlying strata in gob under 3D circumstance.

2.2. Characterization of permeability change of coal and rock under the mining influences

The distribution and evolution law of the permeability of overlying coal and rock under the influence of mining is always the key research content of gas extraction. However, most of researchers treat the permeability of coal and rock as the constant value and do not consider its changes under the influence of mining. They just simply or qualitatively analyze fracture development in local overlying strata of the working face and the permeability change in certain overlying strata (Aksoy et al., 2012), which never gives specific and quantitative descriptions from the perspectives of development and distribution of overlying strata after overall mining and deformation as well as the permeability change (Aksoy et al., 2010).

Researches show that the permeability of coal and rock is actually controlled by porosity in coal and rock as well as increase and decrease in fracture space. The previous research shows that the distribution of mining total strain of overlying coal and rock directly affects the development of fracture (Sheorey et al., 2000), which plays an important role in domination of the change in the porosity of overlying strata. As the key factor, the porosity determines the permeability of coal and rock and gas adsorption.

2.2.1. Total strain and porosity of coal and rock

Coal and rock can be considered as porous media, and extensive researches show the deformation as the sum of the deformation in two parts (Lu et al., 2012; Yu et al., 2014). The first part is body deformation of the media. Because of the deformation caused even by the deformation of skeleton particles of coal and rock, this process is reversible, which is the elastic deformation process. The second part is structural deformation. Because of the deformation caused by the relative dislocation of skeleton particles in spatial structure, this process is usually irreversible.

In the relation between porosity and total strain of coal and rock established below, the slight body deformation of coal and rock is neglected. The analysis and derivation are listed as below:

V_s indicates the solid skeleton volume of porous media, and ΔV_s indicates its change; V_b indicates the bulk volume of porous media, and ΔV_b indicates its change; V_p indicates the pore volume of porous media, and ΔV_p indicates its change.

Defined by the porosity, assuming the porosity of coal and rock under the initial state is as (Eq. 16), (subscript "0" means initial values):

$$\phi_0 = \frac{V_{p0}}{V_{b0}} \tag{15}$$

then coal and rock change from initial state to a certain deformation state, the porosity is as (Eq. 17):

$$\phi = \frac{V_{p0}+\Delta V_P}{V_{b0}+\Delta V_b} = 1-\frac{V_{s0}+\Delta V_s}{V_{b0}+\Delta V_b} = 1-\frac{V_{s0}(1+\frac{\Delta V_s}{V_{s0}})}{V_{b0}(1+\frac{\Delta V_b}{V_{b0}})} = 1-\frac{(1-\phi_0)}{1+\varepsilon_t}(1+\frac{\Delta V_s}{V_{s0}}) \tag{16}$$

In the above Equation, ε_t indicates total strain, and volume strain under 3D condition. The volume changes of unit volume of coal and rock in deformation process, while the strain of coal and rock under 2D condition is the total strain, as shown in (Eq. 15). Neglecting weak body deformation of coal and rock, and setting ΔV_s=0, (Eq. 17) changes to (Eq. 18):

$$\phi = 1 - \frac{(1-\phi_0)}{1+\varepsilon_t} = \frac{\phi_0 + \varepsilon_t}{1+\varepsilon_t} \tag{17}$$

In the above equation, ϕ_0 indicates the original porosity of coal and rock, and ϕ indicates the porosity of coal and rock under the influence of mining. Therefore, the porosity of mining overlying coal and rock can be considered as the function of total strain.

2.2.2. Total strain and permeability of coal and rock

The permeability of coal and rock is a very important physical parameter in the study on the migration of gas, and researchers carry out extensive researches for many years. The permeability of coal and rock varies with the change of the porosity, thus to affect the flow of gas in coal and rock, therefore, the relation of permeability varying with the change of total strain can be obtained with the relationship between permeability and porosity in Kozeny-Carman equation. Kozeny-Carman equation for the relationship between permeability and porosity of coal and rock is as (Eq. 19):

$$K = \frac{\phi}{K_c S_p^{\ 2}} = \frac{\phi^3}{K_c \sum s^2} \tag{18}$$

where:

K_c indicates the constant;

$\sum s$ indicates the porosity surface area in unit volume of porous media, expressed in the following (Eq. 20).:

$$\sum s = \frac{A_s}{V_b} \tag{19}$$

S_p indicates the surface area per pore volume in porous media, expressed in the following (Eq. 21):

$$S_p = \frac{A_p}{V_p} \tag{20}$$

In Eq. (19), A_s indicates total surface area of inner pore of coal and rock. Assume the permeability of coal and rock under the original state is as (Eq. 22):

$$K_0 = \frac{\phi_0^{\ 3}}{K_c \sum s^2} \tag{21}$$

where:

$$\sum s_0 = \frac{A_{s0}}{V_{b0}} \tag{22}$$

When coal and rock change from the original state to a certain deformation state, the accumulated variation quantities of total volume and single media particle are respectively ΔV_b and ΔV_s. Considering coal and rock of specific structure, in the stress-strain process, the total surface area of media particle is approximately considered unchanged. Therefore, the change of pore volume is given by (Eq. 23):

$$\Delta V_p = \Delta V_b - \Delta V_s \tag{23}$$

Therefore, the new porosity is as expressed by (Eq. 24):

$$\phi = \frac{V_p + \Delta V_b - \Delta V_s}{V_b + \Delta V_b} \tag{24}$$

The porosity surface area in new unit volume of porous media is as (Eq. 25):

$$\sum s = \frac{A_{s0}}{V_b + \Delta V_b} \tag{25}$$

In addition, the change of total volume of coal and rock can be obtained from the total strain by (Eq. 26):

$$\Delta V_b = V_b \cdot \varepsilon_t \tag{26}$$

The ratio of new permeability under the influence of mining to the permeability in original state is as (Eq. 27):

$$\frac{K}{K_0} = \frac{\phi^3 \sum s_0^{\ 2}}{\phi_0^{\ 3} \sum s^2} \tag{27}$$

Neglecting weak body deformation coal and rock, setting ΔV_s=0, and substituting Eqs. (25-27) into Eq. (28), the equation of relationship between the change of the permeability and the total strain can be obtained as (Eq. 28):

$$\frac{K}{K_0} = \left(\frac{1 + \frac{\varepsilon_t}{\phi_0}}{1+\varepsilon_t} \right)^3 \tag{28}$$

The above Equation could characterize the change of permeability of coal and rock under the influence of mining, which is the function of total strain of coal and rock.

The total strain can comprehensively reflect mechanical properties and effective stress of coal and rock. Therefore, no matter whether the deformation of coal and rock is elastic or inelastic, linear or nonlinear, (Eq. 29) on the characterization of permeability change could also be used.

3. Case study and results discussion

The studied longwall face is currently mining #15 coal seam in Yangquan Mining area of China. The width of working face is 230 m and the length is 1584 m, the average thickness of coal seam is 6.6m. The maximum mining depth is 526 m, and average mining depth is 468 m. The #15 coal seam is considered as a flat seam.

All overlying strata lithology and relevant physical parameters between immediate roof and topsoil are shown in Table 1.

3.1. Calculation results and analysis of overlying strata movement

In this section, the finial subsidence prediction model for overlying strata of the working face under 3D condition is used, and prediction and analysis are carried out for movement and deformation of overlying strata of the working face. The total strain can comprehensively reflect movement and deformation of overlying strata of the working face under the influence of mining.

Table 1. Values of physical parameters of all overlying strata

Layer number	*Lithology*	*Thickness m*	*Elasticity Modulus GPa*	*Body force MN/m³*	*Tensile strength MPa*	*Poisson ratio*
50	Top soil	2.90	5.00	0.012	0.35	0.30
49	Middle and fine grained sandstone	6.69	29.05	0.022	1.10	0.27
48	Mudstone, limestone	14.58	17.07	0.020	2.50	0.27
47	sandy mudstone	13.31	17.35	0.018	2.00	0.15
46	sandy mudstone	14.32	14.48	0.018	2.00	0.15
45	mudstone	15.47	26.01	0.018	0.61	0.26
44	limestone	7.34	20.90	0.026	3.50	0.25
43	mudstone	5.14	28.79	0.018	0.61	0.26
42	Medium grained sandstone	14.42	32.07	0.022	1.20	0.23
41	limestone	15.64	21.10	0.027	3.50	0.25
40	Middle and fine grained sandstone	12.99	25.87	0.021	1.10	0.27
39	Middle and fine grained sandstone	11.75	28.38	0.023	1.10	0.27
38	Sandy mudstone	9.77	17.21	0.017	2.00	0.15
37	Mudstone	12.90	26.91	0.019	0.61	0.26
36	Limestone	10.75	20.59	0.029	3.50	0.25
35	Mudstone	5.77	28.26	0.020	0.61	0.26
34	Fine sandstone	12.76	28.42	0.024	1.00	0.24
33	Fine sandstone	5.45	26.50	0.026	1.00	0.24
32	mudstone	10.35	27.47	0.020	0.61	0.26
31	limestone	13.28	21.66	0.028	3.50	0.25
30	Limestone and fine-grained sandstone	12.93	24.11	0.024	1.80	0.24
29	mudstone	14.81	27.39	0.018	0.61	0.26
28	Mudstone, limestone	14.26	17.91	0.021	2.50	0.27
27	Fine sandstone	7.30	27.31	0.026	1.00	0.24
26	Limestone and fine-grained sandstone	6.35	18.81	0.024	1.80	0.24
25	Fine sandstone	11.36	27.61	0.024	1.00	0.24
24	Limestone and fine-grained sandstone	6.40	23.17	0.024	1.80	0.24
23	Limestone and fine-grained sandstone	7.70	21.71	0.024	1.80	0.24
22	Coarse grained sandstone	6.77	36.62	0.022	1.00	0.22
21	mudstone	5.15	30.62	0.020	0.61	0.26
20	Medium grained sandstone	8.90	34.28	0.022	1.20	0.23
19	sandy mudstone	13.00	14.39	0.017	2.00	0.15
18	sandy mudstone	14.34	16.03	0.017	2.00	0.15
17	mudstone	14.10	30.33	0.019	0.61	0.26
16	Fine sandstone	6.23	27.19	0.024	1.00	0.24
15	mudstone	7.08	26.54	0.020	0.61	0.26

14	sandy mudstone	11.16	18.95	0.017	2.00	0.15
13	Middle and fine grained sandstone	8.44	28.43	0.022	1.10	0.27
12	sandy mudstone	5.00	18.91	0.017	2.00	0.15
11	Coarse grained sandstone	6.20	39.56	0.020	1.00	0.22
10	Mudstone, limestone	9.07	16.68	0.021	2.50	0.27
9	coal seam	0.50	1.30	0.013	0.60	0.32
8	Medium and fine grained sandstone and mudstone	10.29	26.00	0.019	1.20	0.27
7	coal seam	0.79	1.30	0.013	0.60	0.32
6	Mudstone, limestone, fine sandstone	11.66	21.00	0.018	2.50	0.27
5	coal seam	0.53	1.30	0.013	0.60	0.32
4	Fine sandstone	9.75	27.38	0.024	1.00	0.24
3	mudstone	6.92	27.69	0.020	0.61	0.26
2	Limestone and fine-grained sandstone	6.70	20.32	0.025	1.80	0.24
1	coal seam #15	6.60	16.05	0.016	2.00	0.15

A high total strain value exists in overlying strata within the range of 100m above the coal seam and changes greatly, which has important guidance significance to judgment of existence position and development range of fracture, crack or separation layer. Therefore, in this section, detailed analysis is carried out for distribution law of total strain of overlying strata within the range of 100m above the coal seam under 3D condition, and prediction results of movement and deformation of overlying strata within other height range are only simply displayed and described with figures.

(1) Movement and deformation of overlying strata at the height of 100m, 200m, 300m, 400m and 500m above the coal seam.

Fig. 1 shows that movement and deformation values of overlying strata decrease as the height above the coal seam increases, and the distribution of movement and deformation values has good symmetry. Total strain of overlying strata has a stretch total strain zone around the gob and an inner compress total strain zone; in addition, total strain on both sides of dip in gob is slightly larger than total strain value on both sides of strike (Peng, 2008). However, the overlying strata within a certain height range above the coal seam in dip direction reaches full subsidence state, and only a strike main section exists, thus to cause the difference in movement and deformation of upper overlying strata in strike and dip directions.

(2) Analysis of distribution law of total strain of overlying strata in the height range of 100m above the coals seam under 3D condition

Fig. 2 is the distribution map of total strain of overlying strata at the height of 40m, 50m, 60m, 70m, 80m and 90m above the coal seam. By comparison with Fig. 1(g), it is not difficult to find that high total strain value exists in overlying strata within the height range of 100m above the coal seam, and the following conclusion is reached upon analysis combining the isoline distribution of total strain at the above height in Fig. 2.

The total strain of overlying strata has a stretching total strain zone around the gob and an inner compress total strain zone, and the widths of the above stretching total strain zone and compress total strain zone are different in strike and dip of gob; total strain value decreases as the height above the coal seam increases, and the total strain value on both sides of dip in gob is slightly larger than the total strain value on both sides of strike.

Therefore, total strain of overlying strata is divided into three zones:

- Tensile strain circle (dip width and strike width gradually increase from down to up, but dip width is slightly larger than the strike width; tensile strain circle at the height of 90 m over the coal seam can reach near 0~32 m inside intake airflow roadway and 0~30m inside open-off cut and stopping line in strike; in addition, the tensile strain circle is the weak tensile strain zone at four corners of the gob).
- Compression strain circle (strike width and dip width gradually increase from down to up, but dip width is slightly less than strike width; the compression strain circle at the height of 90m over the coal seam can reach near 32m~50m inside intake airflow roadway and return airway in dip and near 30m~53m inside open-off cut and stopping line in strike).
- Middle pressure relief zone (located in the middle of gob, which gradually decreases from down to up with a weak stretching state).

The total strain can comprehensively reflect movement and deformation of overlying strata of the working face under the influence of mining, which can guide and judge existence position and development range of fracture, crack or separation layer in overlying strata. In addition, positive and negative total strain values respectively reflect the expansion and contraction of rock under the influence of mining, and the positive value represents the strength of gap in rocks, which can reflect the increase of breathability in overlying strata. Therefore, according to distribution law of total strain of overlying strata in gob, overlying strata fractured can be divided into three zones: The annular tensile fracture growth zone (coal and rock stay in the tensile strain circle, fully

expanded and deformed, and mining fracture is developed, and breathability increases, which is main movement and enrichment area for gas); annular compress fracture closure zone (coal and rock stays in the compression strain circle, fracture is contracted and closed by extrusion, with poor breathability and difficulty in gas migration) and middle compaction zone (coal and rock stay in pressure relief zone, mining fracture is almost compacted under the effect of overlying strata pressure, stretching strain value is small and near zero, with poor breathability and difficulty in gas migration). Therefore, 14#, 13#, 12# and 11# coal seam adjacent to 15# mining coal seam as well as surrounding rock K3 and K4 limestone rich in gas (height range is approx. between 43-45m, 46-48m, and 55-58m) have high annular tensile fracture growth zones around the gob, mining fracture development degree is high, and gas desorbs and migrates to the adjacent fracture development surrounding rock.

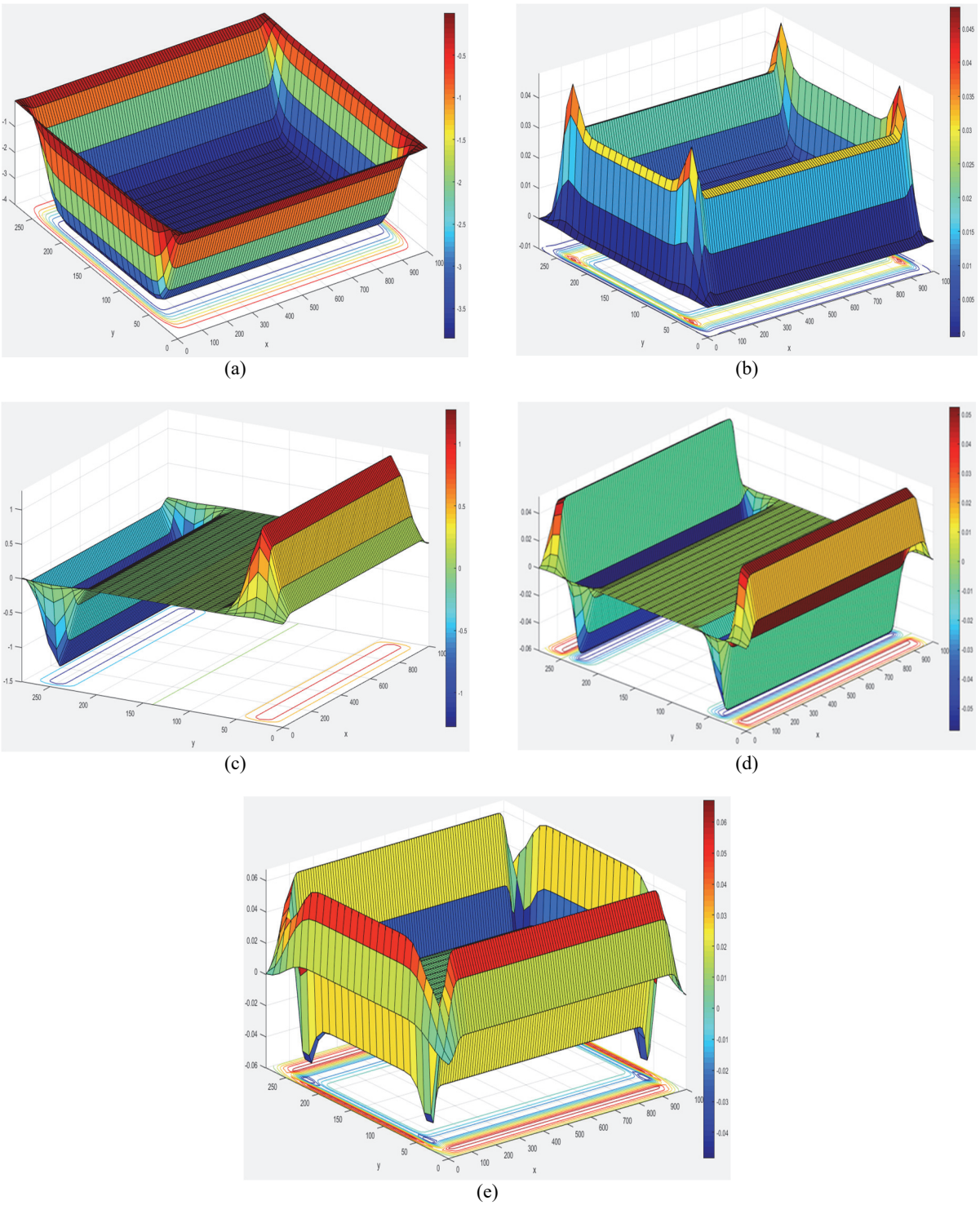

Fig. 1. Calculations of Strata movement and deformation in 100m level over coal seam: (a) vertical subsidence; (b) vertical strain, horizontal displacement in dip direction;(d) horizontal strain in dip direction; (e) Total strain

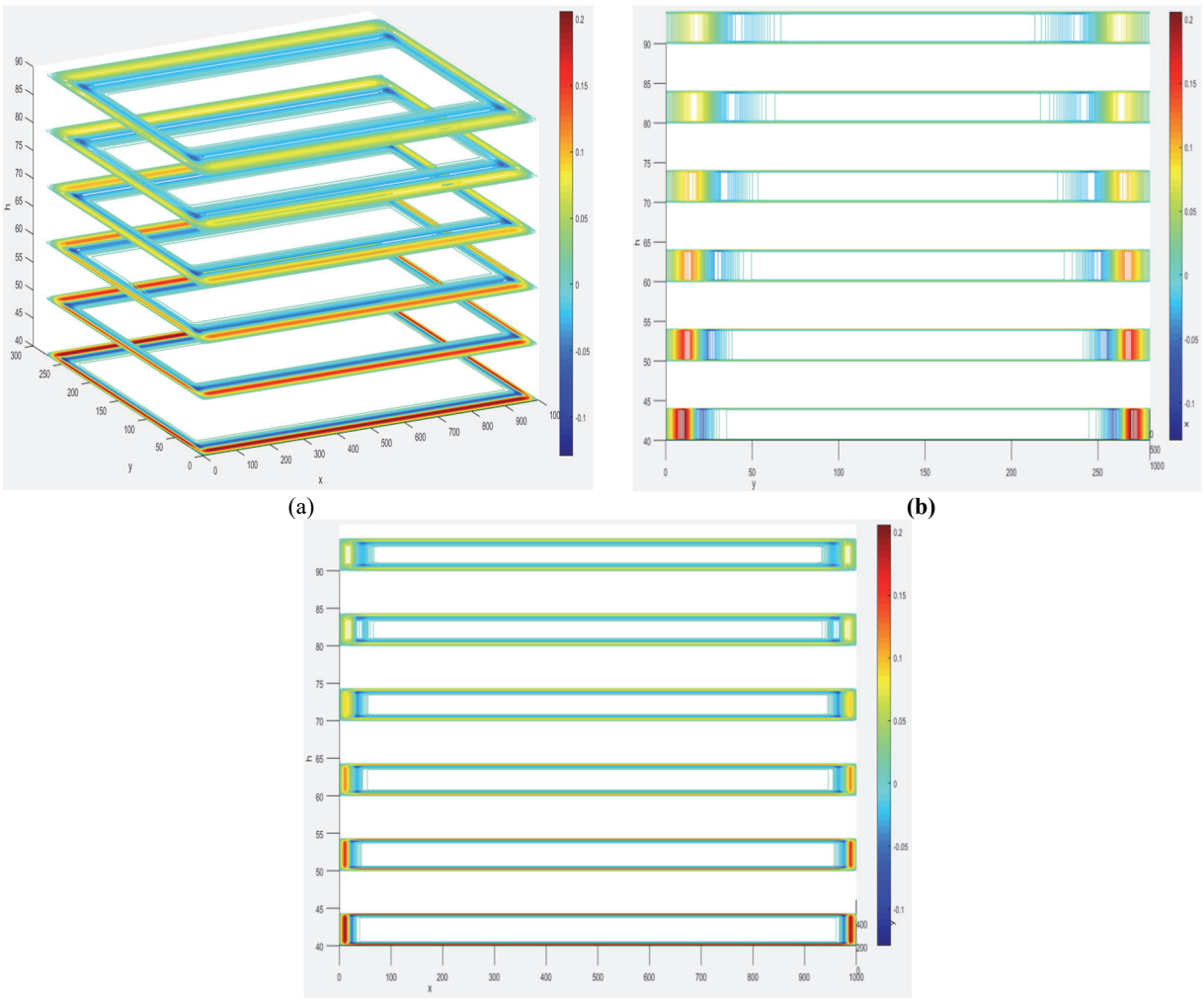

Fig. 2. Total strain distribution in 40m, 50m, 60m, 70m, 80m and 90m over coal seam with different viewing angle: (a) 45° viewing angle; (b) Strike direction view; (c) Dip direction view

3.2. Calculation results and analysis of permeability change of overlying strata

The equation of characterizing change of mining permeability shows that it is only the function of total strain under the condition that the initial porosity of coal and rock is known. The initial porosity of overlying strata of the underground working face is compared and determined upon investigation of relevant literatures and experiences. Overlying strata are reasonably divided into groups according to research needs, overlying strata lithology and thickness. The average porosity of each group is obtained as shown in Table 2 and Table 3.

According to finial 3D subsidence prediction model for overlying strata, Eq. (4) and Eq. (15) as well as original porosity of overlying strata, prediction and analysis of the change of porosity and permeability of overlying strata in gob of test working face under the influence of mining are carried out.

(1) Change of porosity and permeability of mining overlying strata at the height of 100 m, 200 m, 300 m, 400 m and 500 m above the coal seam.

Fig. 3 shows that the change distribution of mining porosity and permeability of overlying strata almost keeps consistent with the distribution of total strain, porosity and permeability of each overlying strata under the influence of mining have an increase area and an inner decrease area around the gob, and the position is almost consistent with the position of stretching total strain zone and compress total strain zone in Section 3.1.

In addition, affected by the total strain, within the height range of over 100m above the coal seam, the change amplitude of porosity and permeability from down to up nearly presents the gradually decreasing trend, and the change amplitude on both sides of dip in gob is larger than the change amplitude on both sides of strike in gob. However, it can be obviously seen that the change amplitude of permeability at the same height is larger than that of the porosity.

(2) Analysis of distribution law of change of the permeability of overlying strata and gas permeation & migration pathway within the height range of 100m above the coal seam.

Table 2. Rock porosity over longwall face

Lithology	***Porosity /%*** Min.-Max. Avg.
Loose soil layer	30.00
Mudstone	4.09-8.80 6.45
Sandy mudstone	6.60
Sandstone	4.20-24.60 13.20
Fine sandstone	2.80-17.50 7.05
Middle sandstone	3.60-7.10 5.35
Coarse sand rock	3.20-15.80 9.50
Siltston	4.60
Limestone	18.00
Coal	6.76

Table 3. Porosity in different strata

Number	***Layer No.***	***Thickness/m***	***Distance over 15# coal seam/m***	***Ave. Porosity/%***
1	50	30.20	511.23	30.00
2	49, 48, 47	11.29	170.83	7.05
3	46, 45	10.05	159.54	5.83
4	44, 43, 42	12.29	149.49	7.21
5	41, 40, 39, 38, 37	12.54	137.20	5.95
6	36, 35	9.38	124.66	5.54
7	34, 33, 32	10.94	115.28	5.15
8	31, 30, 29, 28	13.46	104.34	6.03
9	27, 26, 25, 24, 23	10.68	90.88	6.75
10	22, 21, 20	10.10	80.20	7.43
11	19	11.74	70.10	4.60
12	18, 17, 16, 15	10.44	58.36	8.25
13	14, 13, 12, 11, 10	4.95	47.92	10.57
14	9	16.30	42.97	9.50
15	8, 7	12.30	26.67	9.50
16	6, 5, 4, 3, 2	14.37	14.37	13.35
17	1	6	/	6.76

The change of permeability of mining overlying strata is annular distribution around the gob, and the change of permeability inside intake airflow roadway and return airway is obviously larger than the change of the permeability inside open-off cut and stopping line. According to distribution of isoline, the change of the permeability of mining overlying strata around the gob is divided into three areas: annular permeability increase area, annular permeability decrease area and permeability recovery area, and these three areas are almost same with position and range of tensile strain circle, compression strain circle and middle pressure relief zone of total strain in Section 3.1.

In addition, it is worth noting that the change of the permeability of mining overlying strata within the range of 100m above the coal seam gradually increases from down to up, reaching the maximum value near h=60m, which then gradually decreases. Also, it is worth noting that the change of the permeability of mining overlying strata within the range of 100m above the coal seam gradually increases from down to up, reaching the maximum value near h=60m, which then gradually decreases. Combined with the distribution of mining permeability change in main section in Fig. 4, it can be nearly determined that the annular permeability increase area within a certain range near h=60m has a high permeability increase area.

Fig. 5 shows that it can be determined that the high permeability change area of overlying strata is approximately located within the range of 59m-67m above the coal seam by comparative analysis of the mining permeability change of overlying strata near the height of 60m above the coal seam, and the mining permeability within such range can be 22 times to 37 times the original permeability. The change of mining permeability of overlying strata at the height of h=59m is the maximum, which is 37 times the original permeability, which may be caused by the total strain

value at such height larger than the total strain at other height. Fig. 5 further shows that compared with the annular permeability increases area, the range of annular permeability decrease area is much smaller, and the annular permeability increase area has high permeability change area. However, high permeability change area is not distributed like the annular permeability increase area, but divided into four areas by four corners of the gob, which are respectively located within a certain range inside intake airflow roadway, return airway, open-off cut and stopping line. Specific location is:

- Inside intake airflow roadway and return airway: The dip range is approx. 8m-18m, and the width is approx. 10m; the strike range is approx. 27m-973m, and the length is approx. 946m;
- Inside set-up and recover lines: The strike range is approx. 7m-16m, and the width is approx. 9m; the dip range is approx. 28m-252m, and the length is approx. 224m.

In addition, Fig. 5 shows that the increase amplitude of the permeability of high permeability change area inside intake airflow roadway and return airway is slightly larger than the increase range of the permeability of high permeability change area inside open-off cut and stopping line. From the above analysis, the change distribution of mining permeability under 2D condition is further modified, which can accurately determine the change distribution of the annular permeability of mining overlying strata and annular gas enrichment area, as shown in Figs. 6 and 7.

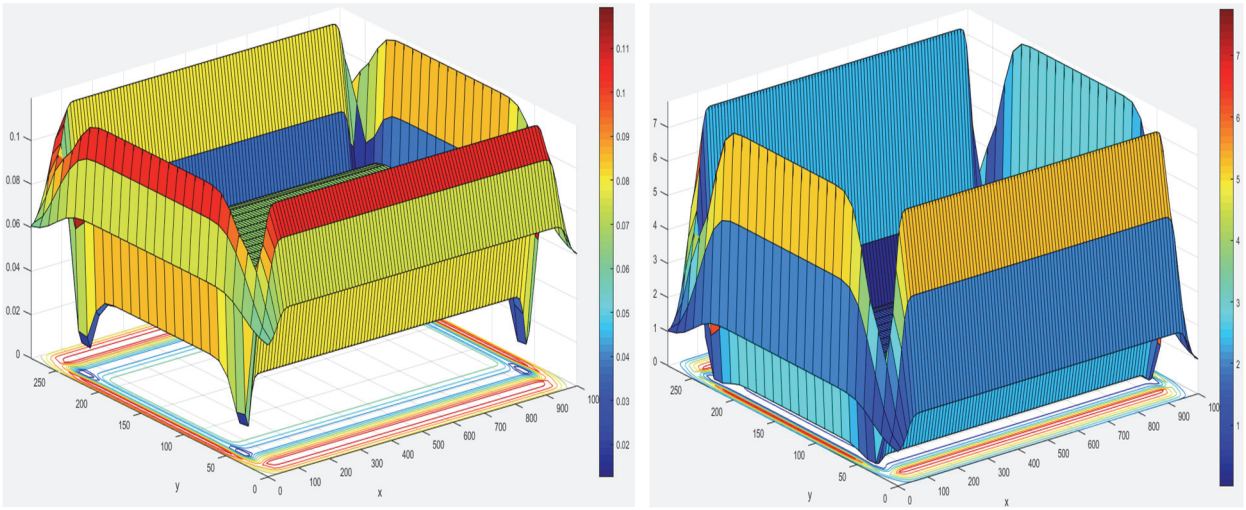

(a) **(b)**

Fig. 3. Porosity and Permeability distribution after mining in 100m over coal seam: (a) Porosity; (b) Permeability

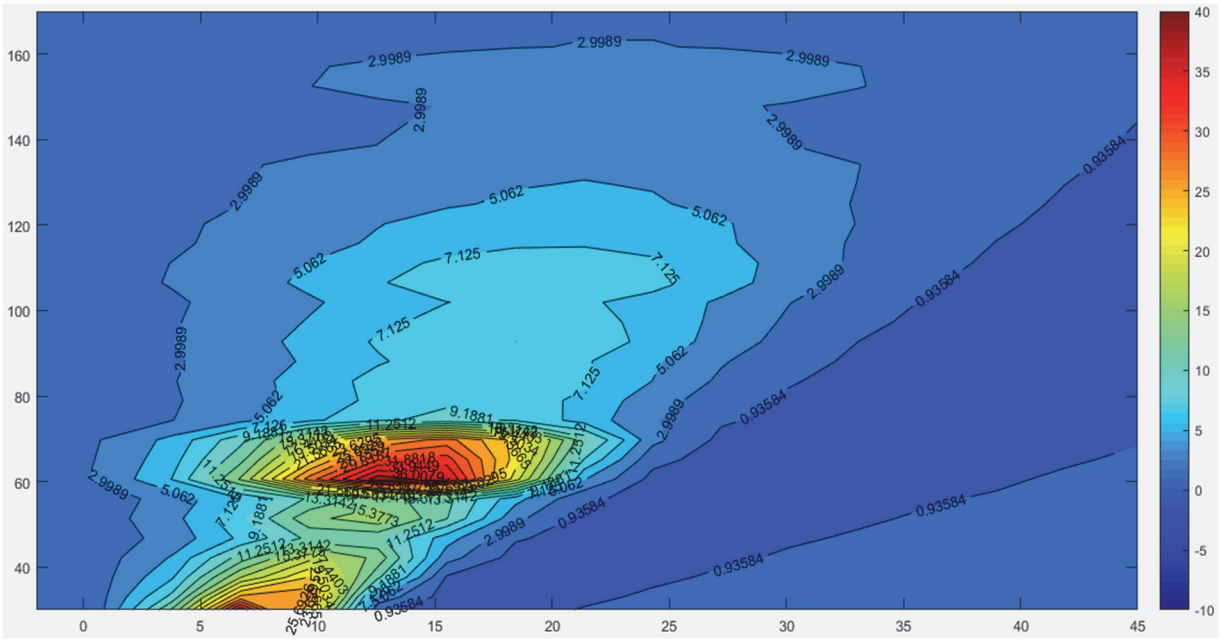

Fig. 4. Permeability distribution of overlying strata (y=-3m~45m, h=30m~170m)

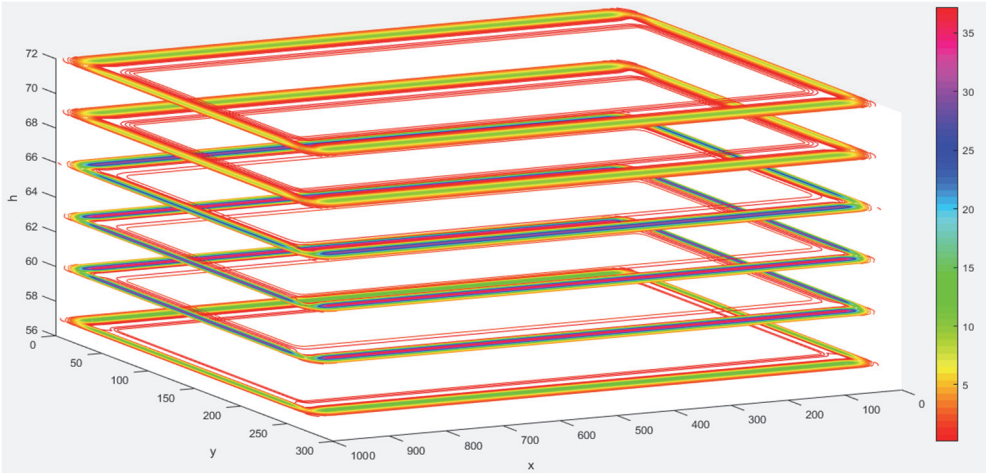

Fig. 5. Isocline of Permeability in 57m, 60m, 63m and 72m over coal seam

The main migration pathway for pressure relief and desorption of gas which migrates from annular permeability decrease area into annular permeability increased area. In addition, a high permeability change area exists inside intake airflow roadway, return airway, open-off cut and stopping line within a certain height range of intake airflow roadway, return airway, open-off cut and stopping line of the annular permeability increase area, and gas for pressure relief and desorption migrates to this area under the effect of seepage motive and rising diffusion, and this area is the "annular" gas enrichment area of mining overlying strata.

3.3 Engineering design of gas extraction scheme of test working face

The above analysis shows that the overlying strata within the range of 7m-20m behind the advancing process of the working face are permeability increasing area, providing channel for permeation and migration of pressure relief gas. In addition, a high permeability change area exists within the range of 58m-67m above the coal seam in the permeability increase area, especially the change of mining permeability at 15m behind the working face and 60m above the coal seam is the maximum, which is the gas enrichment area.

At the same time, the annular permeability increased area around the gob moves forward with advancing of the working face, and a high permeability change area exists within the range of 59m-67m above the coal seam, especially the change of mining permeability of overlying strata at the height of h=59m is the maximum, which is the high-level annular gas enrichment area. The upper coal seam and surrounding rock rich in gas of test working face are 14#, 13#, 12# and 11# coal seam as well as K3 and K4 limestone.

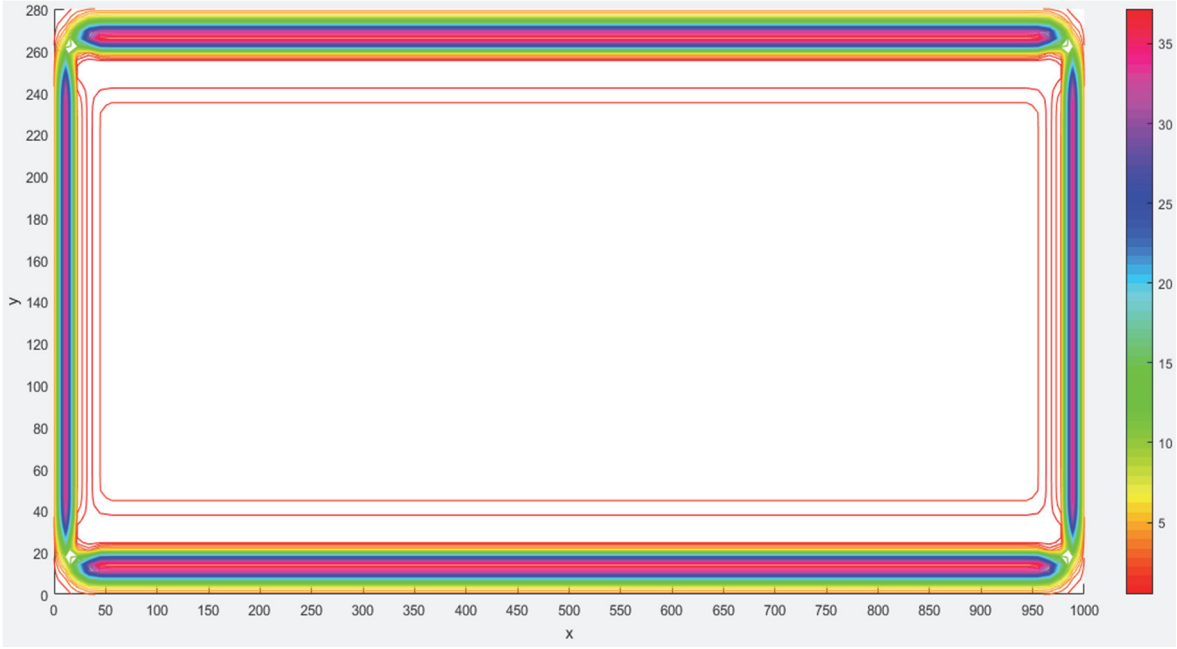

Fig. 6. Permeability distribution after mining at 59m over coal seam

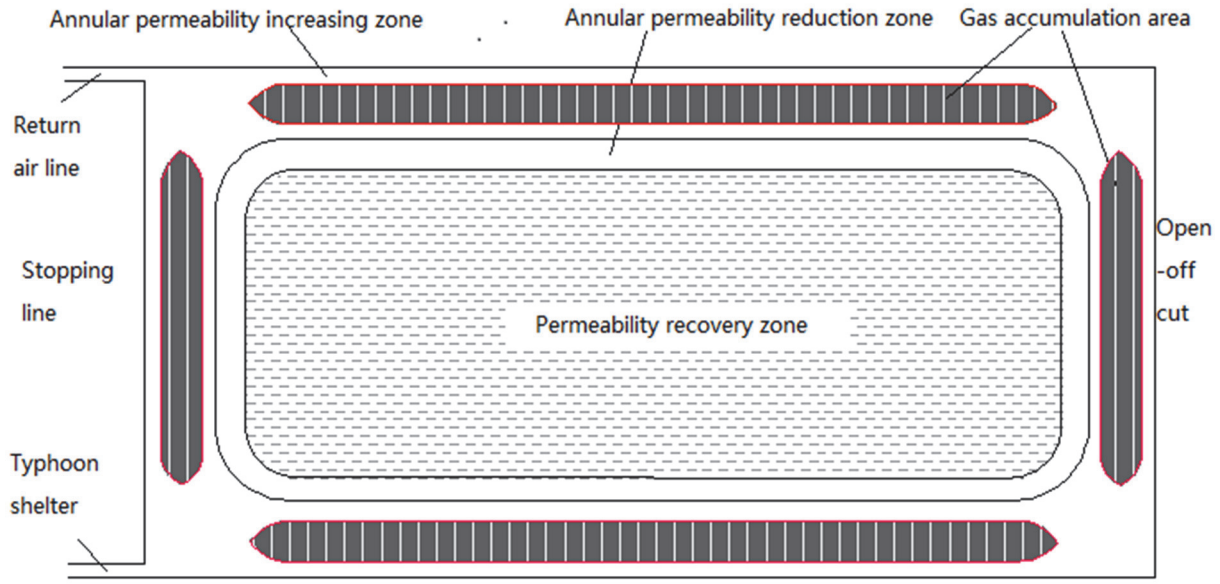

Fig. 7. Permeability change zone and gas enrichment area of overlying strata

The height range is approx. 43-45m, 46-48m and 55-58m, which are in the height range of permeability increase area; in order to solve large influx of pressure relief gas adjacent to coal strata into the working face and gas overrun of the upper corner, the pressure relief gas is extracted and technical parameters are optimized by the following scheme according to change distribution of mining permeability, gas migration and accumulation law:

● Ground drilling: High-concentration and high-content gas in high permeability change area of mining overlying strata is extracted with ground drilling; in order to extract gas efficiently, the surface drilling is located above the permeability increase area, and the plane position is controlled within the range of 8m-18m inside return airway of the working face; final drilling position is located in gas enrichment area, namely, within the range of 58m-67m above the coal seam, the position of drilling strike is located within the range of 15m inside open-off cut and 15m behind the stopping line.

● Layer-through drilling: Gas is extracted through working face roadway by drilling from roof fractured zone to high-level gas enrichment area, and the first extraction drilling field is arranged at 15m inside open-off cut, and a drilling field is arranged every 15m, until at approx. 15m after the stopping line, 3~5 drills are arranged within every drilling field; the final drill is within high-level gas enrichment area, and the drilling elevation coverage is approx. 72°-80°.

● Strike high level drainage roadway: Gas is extracted from a roadway parallel to return airway arranged in roof fractured zone at a certain distance from return airway of the working face, specifically arranged in high-level gas enrichment area at 8m-18m from the return airway and 58m-67m above the coal seam, the plane position at the end of high level suction roadway should be near 15m inside open-off cut; in order to solve the gas emission of the working face of coal seam of initial mining, a rear high level suction roadway can be arranged between strike high level suction roadway and open-off cut.

● Dip high level drainage roadway: A dip roadway is dug along dip towards the gob in outward staggered tail gateway of the working face to the level of high-level gas enrichment area, and a section of drift is dug into the enrichment area to extract the pressure relief gas near the coal strata; the height of dip high level suction roadway should be within the range of 58m-67m above the coal seam, and the plane position at the end of drift should be 8m-18m from the return airway, namely, in high-level gas enrichment area, the first dip high level suction roadway should be arranged near 15m inside open-off cut, after which a dip high level suction roadway is arranged at a reasonable interval. Actually, in mining of coal seam group of Yangquan mining area, the gas emission near coal strata is large, the gas extraction effect by drilling is not good, and the mining pressure relief gas near the coal strata should be extracted with high level suction roadway. While the actual extraction data of Yangquan mining area shows that the average extraction rate of dip high level suction roadway is only 46.19%, and the average extraction rate of gas of strike high level suction roadway can reach 90%, ensuring the safety production of the working face and efficient extraction of gas resources in the mine. In addition, in the above analysis, the permeability in high permeability change area inside intake airflow roadway and return airway is higher than the permeability of high permeability change area inside open-off cut and stopping line. Therefore, compared with other extraction scheme, the extraction of pressure relief gas near coal strata of the working face with strike high level suction roadway will be an efficient gas extraction method.

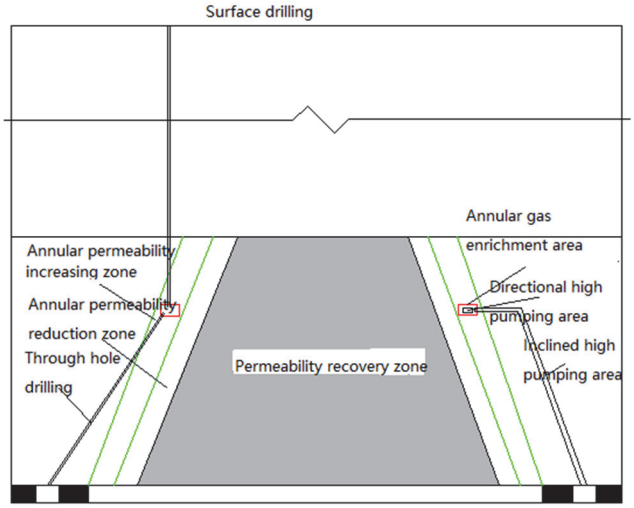

Fig. 8. Scheme of gas extraction methods based on permeability change calculation results

4. Conclusions

In this paper, the research method combines mathematical modeling, theoretical analysis and numerical simulation, to study the gas permeation and migration pathway based on strata movement and deformation over the underground mining working face. With influence function method as the theoretic basis, a finial 3D subsidence prediction model for overlying strata is developed; the concept of 3D total strain and its mathematical expression are proposed. The characterizing equation of the relationship between changes of total strain, porosity and permeability is obtained by deduction, and prediction is carried out for the change of porosity and permeability of mining overlying strata based on total strain.

Under the final subsidence state, the change of the permeability inside intake airflow roadway and return airway is larger than the change of the permeability inside open-off cut and stopping line. It is divided into three areas according to characteristics of the annular distribution of permeability change of mining overlying strata around gob: annular permeability increase area, annular permeability decrease area and permeability recovery area.

Specific position and range of high-level annular gas enrichment area of test working face under the final subsidence state as well as dynamic evolution law of high-level gas enrichment area in the mining process are obtained, gas extraction plan of working face is put forward and technical parameters are optimized.

Acknowledgements

This work is financially supported by grant from Independent Research Projects of State Key Laboratory of Coal Resources and Safe Mining, CUMT (Grant No. SKLCRSM18X002), Fundamental Research Funds for the Central Universities (Grant No.2015XKMS007), Natural Science Foundation of Jiangsu Province of China (Grant No.BK20181355), China Postdoctoral Science Foundation funded project (Grant No. 2015MS581897) and Priority Academic Program Development of Jiangsu Higher Education Institutions. The authors are grateful for the supports.

References

Aksoy C.O., Özacar V., Kantarci O, (2010), An Example for Estimation of Rock Mass Deformations Around an Underground Opening by Numerical Modeling, *International Journal of Rock Mechanics and Mining Sciences*, **47**, 272-278.

Aksoy C., Geniş M., Aldas G., Özacar V., Ozer S., Yılmaz Ö., (2012), A comparative study of the determination of rock mass deformation modulus by using different empirical approaches, *Engineering Geology*, **131-132**, 19-28.

Deng G., (1999), *Study on the effect of rock mass in mining subsidence*, China University of Mining and Technology Press, Xuzhou, China.

Donnelly L., De L., Asmar I., (2001), The monitoring and prediction of mining subsidence in the Amaga, Angelopolis, Venecia and Bolombolo Regions, Antioquia, Colombia, *Engineering Geology*, **59**, 103-114.

Guo W., Huang C., Chen J., (2011), Observation and study on surface ground subsidence speed of fully mechanized top coal caving mining in thick seam, *Coal Science and Technology*, **39**, 114-117.

Han G., Cheng J., Yi G., (2010), Foreign mining subsidence prediction research and application overview of technology, *Chinese Production Safety Technology*, **7**, 41-45.

He G., (1988), Weibull distribution method for prediction of rock movement, *Journal of China University of Mining and Technology*, **10**, 1-20.

He M., (1996), *Utilization of thermal energy stored in underground strata*, National Natural Science Foundation of China Seminar, Beijing, vol.1, 16-19.

Jiang D., Zhang G., Hu Y., (1997), Study on the influence of effective stress on permeability of coalbed methane, *Journal of Chongqing University*, **20**, 22-25.

Li X., Guo Y., Wu S., (2005), Analysis of relation between coal swelling deformation and porosity and permeability, *Journal of Taiyuan University of Technology*, **36**, 264-265.

Liu B., (1992), Theory of stochastic medium and its application in surface subsidence due to excavation, *Stability in Surface Mining*, **13**, 17-24.

Liu B., Liao G., (1965), *The Basic Law of Surface Movement in Coal Mine*, China Coal Industry Press, Beijing.

Liu B., Lin D., (1982), The application of stochastic medium theory to the problem of surface movements due to open pit mining, *Stability in Surface Mining*, **3**, 407-416.

Lu P., Shen Z., Zhu G., (2012), Rock permeability characterization and experimental study in the whole process of strain, *Journal of University of Science & Technology China*, **32**, 678-684.

Minea I., Croitoru A., (2017), Groundwater response to changes in precipitations in North-Eastern Romania, *Environmental Engineering and Management Journal,* **16**, 643-651.

Mostofa A., Quamruzzaman C., (2009), Longwall stress distribution in 1101 coal face of the barapukuria coal mine, Dinajpur, Bangladesh*, Cafetinnova Org*, **2**, 55-62.

Peng S., (2008), *Coal Mine Ground Control*, Wiley, New York.

Peng S., Luo Y., (1992), *Comprehensive and Integrated Subsidence Prediction Model CISPM (V2.0)*, Proceedings of the 3rd Workshop on Surface Subsidence Due to Underground Mining, Morgantown, vol. 1, 22-31.

Qian M., Shi P., Xu J., (2010), *Mining Pressure and Strata Control,* 2nd Edition (in Chinese), China University of Mining and Technology press, Xuzhou, China

Schatze S., Karacan C., Dougherty H., (2012), An analysis of reservoir conditions and responses in long wall panel overburden during mining and its effect on gob gas well performance, *Engineering Geology*, **12**, 65-74.

Sheorey P., Loui J., Singh K., Singh S., (2000), Ground subsidence observations and a modified influence function method for complete subsidence prediction, *International Journal of Rock Mechanics and Mining Sciences*, **37**, 801–818.

Tošović R., Dašić P., Ristović I., (2016), Sustainable use of metallic mineral resources of Serbia from an environmental perspective, *Environmental Engineering and Management Journal,* **15**, 2075-2084.

Wang G., Xue D., Gao H., (2012), Sexangula of coal and rock stress-strain process of seepage characteristics, *Journal of China Coal Society*, **37**, 107-112.

Xie H., Chen Z., (1988), Nonlinear large deformation finite element and its application in rock movement, *Journal of China University of Mining and Technology,* **2**, 94-98.

Xie H., Yang L., Yu G., (1988), Statistical research on joint rock mass subsidence, *The Damage Mechanics and Practice*, **20**, 7-9.

Xue D., Zhou H., Tang X., (2013), Gas coal rock permeability distribution and evolution of mining engineering, *Journal of China Coal Society*, **38**, 930-931.

Yu Y., Zhang C., Zhao Q., (2014), Bearing model and numerical analysis of surrounding rock permeability evolution, *Journal of China Coal Society*, **39**, 841-848.

Zhang Y., (1996), Simulation of strata movements due to underground mining using an automated measurement system for equivalent material modeling facility, *Journal of Coal Science & Engineering*, **2**, 10-15.

Zhang Y., Zhong W., Yao J., (1987), Calculation of dislocation theory of strata movement in the solution and the boundary element method, *Journal of China Coal Society*, **2**, 27-33.

Zhao W., Meng Q., (2010), The history and trend of research on mining subsidence at home and abroad, *Journal of Beijing Polytechnic College*, **9**, 12-15.